Comparison of Different Formulations for Eddy-Current Computations in an Induction Furnace

D. van Riesen and G. Henneberger
Department of Electrical Machines (IEM),
Aachen University (RWTH Aachen)
Schinkelstraße 4
D-52064 Aachen, Germany
e-mail: dirk.vanriesen@iem.rwth-aachen.de

C. Kaehler
Bosch Rexroth AG
Department for Electric Drives and Controls
Bgm.-Dr.-Nebel-Straße 2
D-97816 Lohr, Germany
e-mail: christian.kaehler@boschrexroth.de

Abstract

Eddy-current computations are becoming more commonly used as both, the computational power and the demand for more accurate eddy-current loss estimation increase. Several different formulations for the calculation of eddy currents using the finite-element method are known [1]. For industrial applications such as induction furnaces or claw-pole alternators, fast and reliably stable models are required. This paper compares different formulations based on the use of the magnetic vector potential with regard to the stability of the convergence.

Formulations

A very thorough overview over different formulations for eddy-current computations is given in [1], with a focus on a time-harmonic model. For the simulation of electrical machines, formulations using the magnetic vector potential A are most commonly used. The eddy currents are taken into account using either the electric scalar potential V, the electric vector potential T or only the time derivative of the magnetic vector potential. The $A-A,V$ formulation is generally considered to be the best in terms of stability and convergence rate. The Galerkin formulation for the time-harmonic model reads:

$$\int_{\Omega_n,\Omega_c} \nabla\times\breve{N}_i\cdot\nu\nabla\times\breve{A}\,d\Omega+\int_{\Omega_c} j\omega\sigma\breve{N}_i\cdot\breve{A}\,d\Omega+\int_{\Omega_c} j\omega\sigma\breve{N}_i\cdot\nabla\cdot V\,d\Omega=\int_{\Omega_n,\Omega_c}\nabla\times\breve{N}_i\cdot\breve{T}_0\,d\Omega\quad\forall\breve{N}_i \tag{1}$$

$$\wedge\int_{\Omega_c} j\omega\sigma\nabla\cdot N_i\cdot\breve{A}\,d\Omega+\int_{\Omega_c} j\omega\nabla\cdot N_i\cdot\nabla\cdot V\,d\Omega=0\quad\forall N_i \tag{2}$$

Ω_n denotes regions without eddy currents. Ω_c denotes eddy-current regions. If only short-circuited eddy-current regions exist in the model. Equation (2) and the term involving the electric scalar potential can be eliminated, resulting in the A formulation. The equations (1) and (2) can be transformed into the time domain for a transient model, using the Galerkin scheme [2], resulting e.g. for the magnetic vector potential in:

$$\mathring{A}(t)=(1-\tau)\mathring{A}_n+\tau\,\mathring{A}_{n+1},\quad \tau=\frac{t-t_n}{t_{n+1}-t_n}=\frac{t-t_n}{\Delta t},\quad \frac{\partial A(t)}{\partial t}=\frac{A_{n+1}-A_n}{\Delta t} \tag{3}$$

$\tau=2/3$ according to the Galerkin scheme. With this, the transient form of the $A-A,V$ formulation yields:

$$\begin{aligned}&\int_{\Omega_n,\Omega_c}\tau\,\nabla\times\mathring{N}_i\cdot\nu\nabla\times\mathring{A}_{n+1}\,d\Omega+\int_{\Omega_c}\frac{\sigma}{\Delta t}\mathring{N}_i\cdot\mathring{A}_{n+1}\,d\Omega+\int_{\Omega_c}\frac{\sigma}{\Delta t}\mathring{N}_i\cdot\nabla\cdot V_{n+1}\,d\Omega=\\&\int_{\Omega_n,\Omega_c}\nabla\times\mathring{N}_i\cdot\left(\tau\mathring{T}_{0,n+1}+(1-\tau)\mathring{T}_{0,n}\right)d\Omega+\int_{\Omega_c}(\tau-1)\nabla\times\mathring{N}_i\cdot\nu\nabla\times\mathring{A}_n d\Omega+\int_{\Omega_c}\frac{\sigma}{\Delta t}\mathring{N}_i\cdot\mathring{A}_n\,d\Omega+\\&\int_{\Omega_c}\frac{\sigma}{\Delta t}\mathring{N}_i\cdot\nabla\cdot V_n\,d\Omega\quad\forall\mathring{N}_i\end{aligned} \tag{4}$$

$$\wedge \int_{\Omega_c} \frac{\sigma}{\Delta t} \nabla \cdot N_i \cdot \overset{\circ}{A}_{n+1}\, d\Omega + \int_{\Omega_c} \frac{\sigma}{\Delta t} \nabla \cdot N_i \cdot \nabla \cdot V_{n+1}\, d\Omega = \int_{\Omega_c} \frac{\sigma}{\Delta t} \nabla \cdot N_i \cdot \overset{\circ}{A}_n\, d\Omega + \int_{\Omega_c} \frac{\sigma}{\Delta t} \nabla \cdot N_i \cdot \nabla \cdot V_n\, d\Omega \; \forall N_i \quad (5)$$

The $A-A,T$ formulation for the transient model reads:

$$\int_\Omega [\tau\ \nabla \times N_i \nu\ \nabla \times A_{n+1} - \tau\ N_i \nabla \times T_{n+1}]\, d\Omega = \int_\Omega [(\tau-1) \nabla \times N_i \cdot \nu\ \nabla \times A_n - (\tau-1) N_i \nabla \times T_n + \tau\ N_i J_{0n+1} + (\tau-1) J_{0n} + \nabla \times N_i \nu (\tau\ B_{rn+1} + (1-\tau) B_{rn})]\, d\Omega \quad \forall N_i \quad (6)$$

$$\int_\Omega (\tau \nabla \times N_i \cdot \frac{1}{\sigma} \nabla \times T_{n+1} + \nabla \times N_i \cdot \frac{1}{\Delta t} A_{n+1})\, d\Omega = \int_\Omega ((\tau-1) \nabla \times N_i \cdot \frac{1}{\sigma} \nabla \times T_n + \nabla \times N_i \cdot \frac{1}{\Delta t} A_n)\, d\Omega \quad \forall N_i \quad (7)$$

These formulations are implemented in an open-source software package (iMOOSE [3]). For the solution of the system of equations, solvers from the ITL-Package [4] are used. For the symmetric case (all time-harmonic models and all transient except for the $A-A,T$ formulation) a CG solver with Cholesky preconditioning is used. For the transient $A-A,T$ different preconditioner/solver combinations are possible, e.g. BiCG with ILU preconditioner.

Results

The different formulations are applied to the simulation of an induction furnace. Figure 1(a) shows the mechanical model of the device. A crucible containing the melt is surrounded by a coil. 12 yoke parts are located behind the coil to guide the magnetic flux and protect the steel construction of the furnace against stray fluxes and undesired eddy currents. For the electromagnetic calculation, only the relevant parts – melt, coil and yoke – are modeled as a 30° section due to the symmetry of the device.

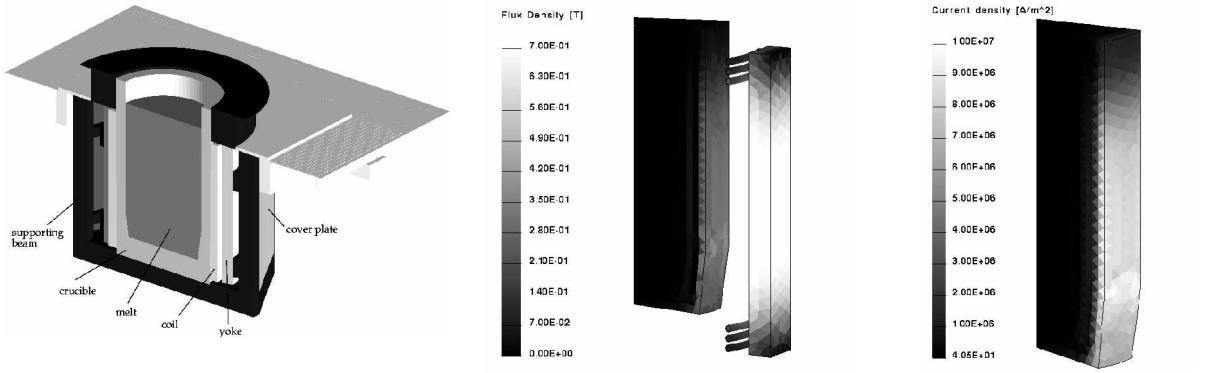

(a) The induction furnace (b) Flux density solution (c) Current density solution (in the melt)

Figure 1: The induction furnace (a), flux density (b) and current density (c) solutions.

The electromagnetic mesh consists of about 475,000 first order tetrahedra. A current is imposed in the coil windings. The melt is modeled as an eddy-current region with a conductivity of $8.33e+5\,(\Omega m)^{-1}$. The operating frequency of the induction furnace is 250 Hz, the coil current 18 kA. All tested formulations yield similar numerical results.

Figure 2 shows the convergence behavior of the three different formulations for the time-harmonic model. The number of unknowns and the number of CG steps required to achieve a relative residuum of 10^{-7} are summarized in Table 1. It can be seen that, as expected, the $A-A,V$ formulation gives the fastest convergence, while the $A-A,T$ formulation needs the highest number of CG steps, which combined with the highest number of unknowns gives the longest computation time.

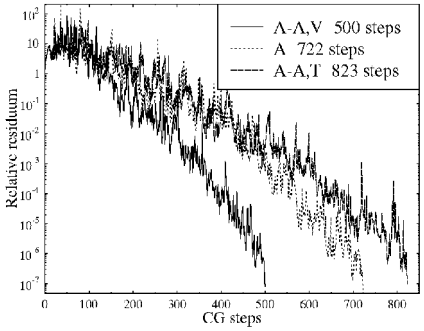

Figure 2: Convergence plot for the time harmonic model.

Formulation	# Unknowns	# CG Steps
$A-A,V$	573.581	500
A	571.982	722
$A-A,T$	580.997	823

Table 1: Nr of unknowns and CG steps for the different formulations.

In the next step the operating frequency is varied. Additionally 50 Hz and 1 kHz are calculated. The results are summarized in Figure 3. Figure 4(a) shows the convergence behavior of all three formulations for a higher conductivity ($4.0e+6\,(\Omega m)^{-1}$) in the melt.

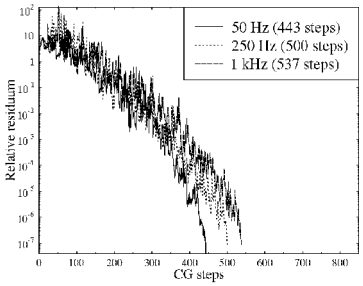

(a) $A-A,V$ formulation

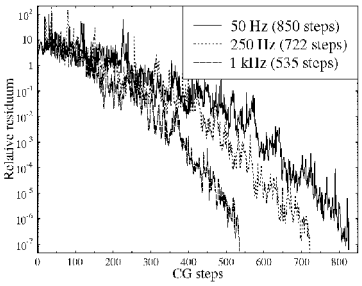

(b) A formulation

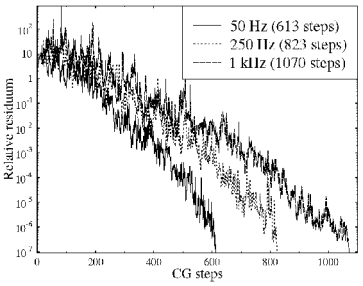

(c) $A-A,T$ formulation

Figure 3: Convergence behavior at different frequencies for $A-A,V$ (a), A (b) and $A-A,T$ (c) formulation.

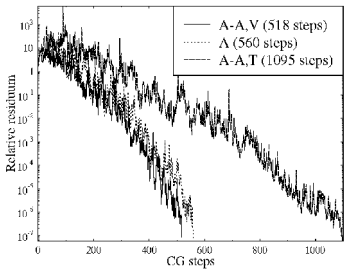

(a) Melt conductivity $4.0e+6\,(\Omega m)^{-1}$

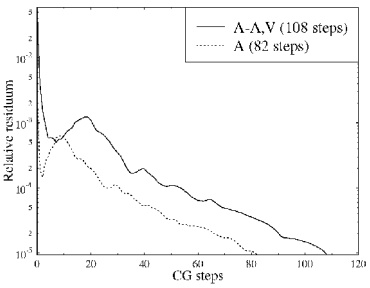

(b) Convergence of transient model

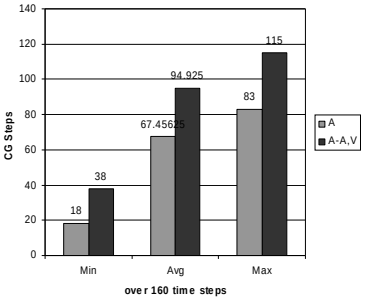

(c) No of CG steps over time steps for transient model

Figure 4: Convergence behavior for a higher melt conductivity (a) and the transient model (b,c).

The results behave in the expected way. The $A-A,V$ formulation shows only a slightly higher number of CG steps at increasing frequencies or conductivity. The A formulation gives better convergence rates at higher frequencies. This is due to the fact, that at the boundaries of the eddy-current region, the condition $J_n = 0$ is only a natural boundary condition and not an enforced one and thus easier satisfied with a large jump in the conductivity. The $A-A,T$ formulation needs more CG steps to converge, especially at higher frequencies. For the transient model though, the A formulation gives a faster convergence for all time steps, as depicted in Figure 4(b) and (c).

Another tested device is the TEAM Workshop problem No. 7 [5]. Figure 5(a) shows the model with the simulated flux density distribution. Figure 5(b) shows the very good agreement between the measurement results provided by [5] and the simulation results, both with the time-harmonic and the transient model. The convergence behavior is plotted in Figure 6. The $A-A,T$ formulation cannot be used here since the eddy-current region is multiply connected.

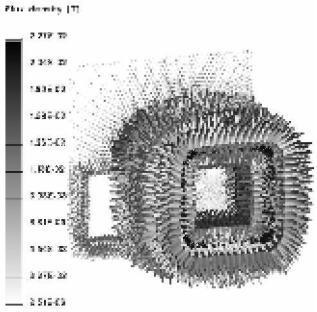

(a) Flux density distribution

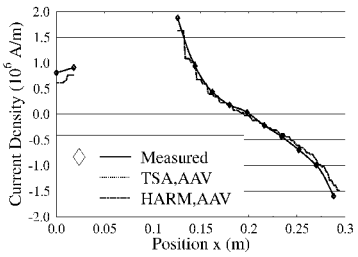

(b) Current density along line

Figure 5: Team No. 7 Workshop problem. Flux density distribution (a) and current density along a line (b).

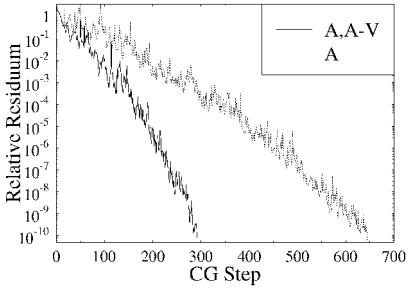

(c) Convergence for harmonic model

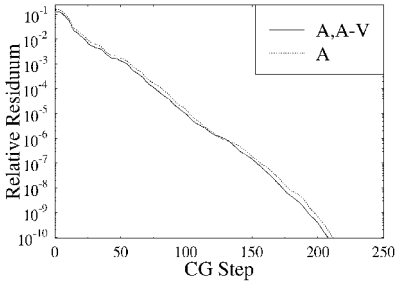

(d) Convergence for transient model

Figure 6: Convergence behavior of the time-harmonic (a) and transient simulation (b) of Team07 Workshop problem.

The results for the time-harmonic model again show the superiority of the $A-A,V$ formulation in terms of fast convergence. Nevertheless, for the transient model there is no difference in the convergence rate between both formulations. Combined with the higher number of unknowns in the case of the $A-A,V$ formulation it results in a larger computation time and thus a disadvantage of the $A-A,V$ formulation.

Conclusion

In this paper three different formulations for eddy-current computations have been compared, both for a time-harmonic and a transient model. The formulations have been applied to the simulation of an induction furnace and the TEAM Workshop problem No. 7. The combination of a magnetic vector potential with an electric scalar potential gives the best and most stable convergence rate in most of the cases, especially for the time-harmonic model. This does not always hold true for the transient case. The reason of this difference has to be further studied.

REFERENCES

1. O. Bíró, "Edge element formulation of eddy current problems", Comput. Methods Appl. Mech. Engrg., vol. 169, pp. 391-405, 1999.
2. O. Zienkiewicz, R. Taylor, „The finite element method", vol. 1, McGraw-Hill Book Company, London 1989.
3. G. Arians, T. Bauer, C. Kaehler, W. Mai, C. Monzel, D. van Riesen, and C. Schlensok, "Innovative Modern Object-Oriented Solver Environment – *i*MOOSE," *Available: http://www.imoose.de*.
4. A. Lumsdaine, J. Siek, L. Lee, "ITL, the iterative template library", http://www.osl.iu.edu/research/itl.
5. K. Fujiwara, T. Nakata, "Results for benchmark problem 7 (asymmetrical conductor with a hole)", Compel, vol. 9, no. 3, pp. 137-154, April 1990.

The effects of the types of elements on the flux and eddy-current distributions are investigated using the A- phi method and the T-Omega method. It is concluded that the brick edge element is best from the viewpoints of accuracy and CPU time.< > Published in: IEEE Transactions on Magnetics (Volume: 26 , Issue: 2 , March 1990).Â 2. L. R. Turner, K. Davey, C. R. I. Emson, K. Miya, N. Nakata, A. Nicolas, "Problems and Workshops for Eddy Current Code Comparison", IEEE Trans. Magnetics, vol. MAG-24, no. 1, pp. 431, 1988. View Article Full Text: PDF (302KB) Google Scholar. 3. A. kameari, "Results for Benchmark Calculations of Problem 4 (the FELIX Brick)", COMPEL, vol. 7, no. 1-2, pp. 65, 1988. CrossRef Google Scholar. 4. , TEAM Workshops: Test Problems, 1988-April. @inproceedings{Riesen2004ComparisonOD, title={Comparison of Different Formulations for Eddy-Current Computations in an Induction Furnace}, author={Dirk van Riesen and Gerhard Henneberger}, year={2004} }. Dirk van Riesen, Gerhard Henneberger. Published 2004. Eddy-current computations are becoming more commonly used as both, the computational power and the demand for more accurate eddy-current loss estimation increase. Several different formulations for the calculation of eddy currents using the finite-element method are known [1]. For industrial applications such as induction furnaces or claw-p Eddy-currents are induced currents that originate, for example, in a moving conductor in a constant magnetic field or in a stationary conducting material subjected to a time-dependent magnetic field. According to [1], the term â€œeddyâ€ originates from the fact that these induced currents create magnetic field vortices inside the conductors.Â Induction furnace: The rapid variation in the magnetic field generates very large eddy-currents, and the heat produced is sufficient to melt a metal; Electric brakes: The brakes expose the wheels (metal) to a magnetic field, which generates eddy-currents.Â A comparison study based on the hysteresis loss of different PMs (i.e., ferrite, samarium-cobalt, and neodymium PMs) has been established [60].